EQUILIBRIUM BEACH PROFILES: U.S. ATLANTIC AND GULF COASTS

By Robert G. Dean

Ocean Engineering Report No. 12
January, 1977

DEPARTMENT OF CIVIL ENGINEERING
UNIVERSITY OF DELAWARE
NEWARK, DELAWARE

TABLE OF CONTENTS

LIST OF FIGURES

LIST OF TABLES

ABSTRACT

Three plausible mechanisms are reviewed which could govern the form of equilibrium beach profiles in the surf zone. The mechanisms considered are: (1) Uniform average longshore shear stress, (2) Uniform average wave energy dissipation rate per unit plan area, and (3) Uniform average wave energy dissipation rate per unit water volume. Each of these mechanisms results in a profile of the power law form with a priori unknown scale and shape parameters; the shape parameter (exponent) depends on the particular mechanism. A set of 502 beach profiles extending from Long Island to the Texas-Mexico border is utilized to determine the shape and scale parameters for each profile. The results suggest that mechanism (3) above may govern and, on this basis, a procedure is presented for calculating the equilibrium beach profile for a sediment of given stability characteristics. The method is illustrated by an example calculation for beach sands of two different diameters.

KEY WORDS: coastal engineering, beach profiles, sediment transport, waves, beach nourishment.

REFERENCE: Dean, R. G., "Equilibrium Beach Profiles: U.S. Atlantic and Gulf Coasts"

EQUILIBRIUM BEACH PROFILES: U.S. ATLANTIC AND GULF COASTS

by

Robert G. Dean, M. ASCE

INTRODUCTION

A knowledge of the characteristics of beach profiles in nature and the relation to the molding action of waves and currents for sediments of differing characteristics is important to a number of coastal engineering problems. For example, beach nourishment comprises the placement of large quantities of sand to advance the shoreline seaward, and is presently widely regarded as the most effective method for alleviating beach erosion. Available methods are not adequate to predict the profile for a certain type of placed material which is different from the native. For example, if the placed material is finer than the native, then through onshore-offshore transport processes, the placed material will form a milder slope than the native and less benefit from the nourishment may be realized than anticipated. The response of beach profiles during periods of increased storm tide and wave height also depends on the stability characteristics of the material. Additionally, sorting of the beach material with the coarser fraction generally migrating toward the beach face and the finer material transported seaward is an important process

[1]Professor, Department of Civil Engineering and College of Marine Studies, University of Delaware, Newark, Delaware 19711.

to understand in coastal engineering problems and designs. If the sediment size distribution is distinctly bimodal, the coarser sediment may be collected into the berm with a steep beach face, with the finer material forming a broad mildly-sloping terrace extending from the beach face through the surf line. As a final example, the gradual response of the shoreline to the slow rise of sea level is of concern in planning beach nourishment projects and the associated maintenance requirements. In particular, it is necessary to know the seaward depth limit to which the transport processes are operative in responding to this rise. Knowledge of this limit and the response of sediments to increasing tide level is necessary to a rational comparison of the relative merits of beach nourishment and oceanic overwash.

This paper reviews three plausible mechanisms, each of which leads to an analytical equilibrium beach profile of the power form. The analytical profile includes two unknown parameters. A data base of 502 beach profiles extending from Long Island around the Florida Peninsula to the Texas-Mexico border is utilized to evaluate the parameters in the beach profiles. The analysis includes a measure of the goodness-of-fit of the analytical profiles and histograms of their parameters. Profiles are grouped according to geomorphic units and averaged and their parameters determined. The data suggest that one of the parameters is a constant value and an interpretation of the analysis results is presented in terms of the dominant operative processes in the surf zone. A parameter is proposed representing the "stability" characteristics of sediment particles with differing fall velocities. Finally, an example is presented of the calculation of two equilibrium beach profiles for sediments of different fall velocities.

BACKGROUND

The subject of equilibrium beach profiles has been of continued interest to geologists and engineers due to applications of interpreting past and present shoreline processes and response of the beach profile and planform to construction along or modification of the shoreline (3,4) (5), (7), (8). The stability of placed material in large beach nourishment projects is intimately related to the equilibrium profile associated with that material and the prevailing wave conditions. There have been a number of laboratory studies (11), (12), (13) of the general characteristics of equilibrium beach profiles and of problems inherent in scaling such results to natural beaches.

Fenneman (7) has presented a qualitative analysis of the various mechanisms which shape the loose granular materials into an equilibrium beach profile. The waves tending to transport material onshore and the return flow ("undertow") currents are regarded as the primary agents in the shaping of the equilibrium beach profile. Fenneman concludes that due to the increase of flow cross-section (depth) offshore, the slope will decrease until the transported material is deposited on the platform on which the wave-built terrace is constructed. The resulting profile would be concave upwards near to shore and concave downward in the seaward portion of the subaqueous terrace.

Keulegan and Krumbein (9) have investigated the characteristics of a mild bottom slope such that the waves never break but rather are continually dissipated by energy losses due to bottom friction. Using solitary wave theory and a value for the kinematic eddy viscosity, a theoretical beach

profile is developed. The slope of the profile is extremely mild. As a particular example, a depth of 13.1 ft (4m) would occur at a distance of 24.9 miles (40 km) from shore. It is concluded that such conditions exist, but are not prevalent along present-day shorelines. The theory may provide explanation for some sedimentary formations which appear to have developed in ancient shallow seas in the absence of breaking wave action.

Bruun (3) has presented an analysis of beach profiles along the Danish North Sea Coast and Mission Bay, California. Beach planforms and profiles along the southern and northern barriers adjacent to Lime Bay, Denmark, are presented dating back to 1874. On the basis of erosion rates at various distances from shore, Bruun developed the following empirical equation between water depth, h, and distance, x, from the shoreline

$$h = A\, x^{2/3} \tag{1}$$

Bruun also proposed two mechanisms leading to an equilibrium beach profile. He first considered the onshore component of shear stress to be uniform, and the onshore component of the gradient of transported wave energy to be constant. This led to an approximate equation of the form found empirically (Eq. 1). Bruun's second mechanism is based on the consideration that the loss of wave energy is due only to bottom friction and that the loss per unit area is constant. Incorporating friction factor results determined in laboratory studies by Bagnold (1), and using a nonlinear wave theory, Bruun found the beach profile to be

$$h = A' \frac{x^{2/3}}{T^{4/9}} \tag{2}$$

Based on considerations of a balance between gravitational and fluid forces, Eagleson, et al. (6) have developed a relationship for the equilibrium beach profile seaward of the breaker zone. The predictions of the method are compared with experimental results and found to be in generally good agreement.

Hayden, et al. (8) have applied an eigenvector method of analysis to identify characteristic forms of 504 beach profiles along the Atlantic and Gulf of Mexico shorelines. This method identifies component features which are common to all profiles in the data set. Analysis of 504 beach profiles resulted in 87 percent of the total variance being described by the first three eigenvectors. This approach is purely descriptive and does not seek to address the processes associated with the forms of the beach profiles.

Dean (5) has presented plausible mechanisms which lead to equilibrium beach profile forms. The physical considerations are based on recognizing that there are both "constructive" and "destructive" forces present in the surf zone which tend to transport sand onshore and offshore, respectively. Without specifically identifying the constructive forces, it is helpful to regard a sand of particular size and specific gravity as stable under a given level of destructive forces. The three destructive forces considered are: (1) Longshore shear stress, using the radiation stress concepts developed by Longuet-Higgins (10) ; (2) Turbulence resulting from transfer of organized wave energy into the more chaotic turbulent water velocity fluctuations; and considering the energy dissipation per unit plan area to be uniform, and (3) Turbulence, considering the wave energy dissipation per unit water volume to be uniform. All of these analyses are based on linear wave theory which

seems reasonable considering the somewhat surprising recent successes (2)(10) in applying this theory to other surf zone problems and in view of the many complexities of the surf zone which preclude complete and accurate representation. These three developments are presented briefly in Appendix III and all yield an equilibrium profile of the form

$$h = A\, x^m \tag{3}$$

in which A is a shape factor, depending on the stability characteristics of the bed material and, as presented in Table I, the value of the exponent, m, depends on the type of destructive force considered.

TABLE I

Value of Exponent m in Eq. (3)

Type of Destructive Force Considered	Value of m
Uniform Longshore Shear Stress	0.4
Turbulence Resulting From Uniform Wave Energy Dissipation Per Unit Plan Area	0.4
Turbulence Resulting From Uniform Wave Energy Dissipation Per Unit Water Volume	0.67

The beach profile described by Eq. (3) varies from concave upward ($m < 1$) to a linear profile ($m = 1$) to convex upward ($m > 1$). Figure 1 presents the general characteristics of the profile types represented by Eq. (3); in this figure, the seaward distance has been normalized by the surf zone width, W, and the depth normalized by the breaking depth, h_b, at the surf line.

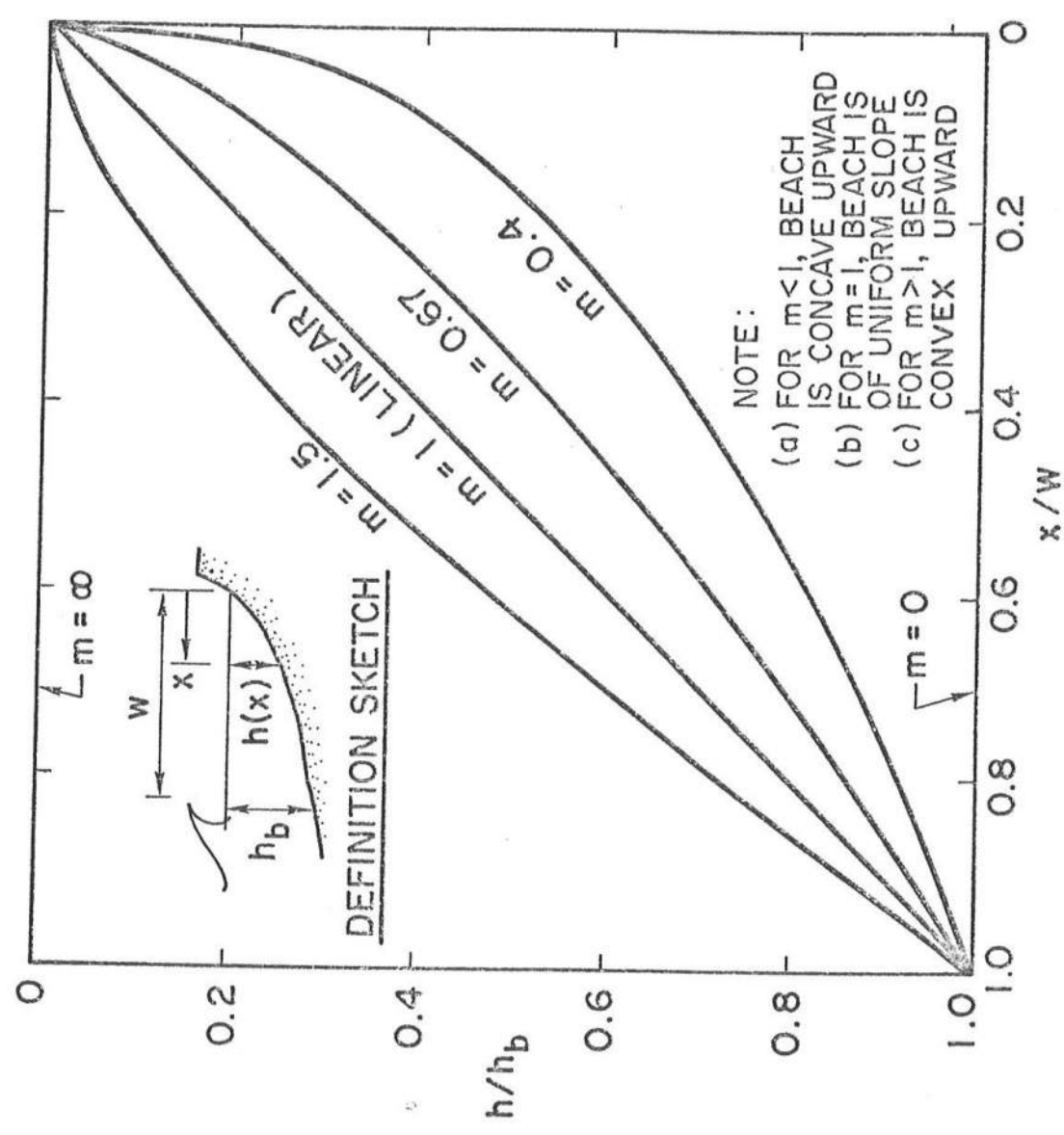

FIGURE 1 CHARACTERISTICS OF DIMENSIONLESS BEACH PROFILE $\frac{h}{h_b} = (\frac{x}{W})^m$ FOR VARIOUS m VALUES

It is recognized that any one or a combination of the mechanisms reviewed herein (or others) could be operative and effective in shaping the equilibrium beach profile. A primary purpose of this paper is to attempt to draw conclusions regarding the dominance of the destructive forces through the evaluation of the shape characteristics of a number of natural beach profiles.

DATA

The data included in the analysis were 502 beach profiles from the United States East Coast and Gulf of Mexico. These profiles are described in Hayden, et al. (8) and were kindly made available to the author by Dr. John Fisher. The profiles span from the eastern end of Long Island to the Texas-Mexico border, see Figure 2. The profile data are presented as depths on 50 ft (15.2 m) spacing and are generally available for a 1200 ft (365.9 m) distance offshore. The preferred elevation datum is Mean Low Water (MLW); however, some profiles are referred to Mean Sea Level or Mean High Water. These differences in elevation datums are not regarded as being of significance to the results obtained from the profile data.

The developments presented briefly in Appendix III result in a beach profile of the form

$$h = A\, x^m \tag{4}$$

where, as noted previously, A is a "scale factor" and m is a "shape factor" with the beach being concave or convex upward depending on whether $m < 1$ or $m > 1$, respectively. Based on several simple considerations for spilling breaking waves across the surf zone, the exponents were found to be 0.4 and 0.67, see Appendix III. The purposes of the data analyses are: (1) to determine how well Eq. (4) represents each data set (profile) and (2) to determine the "best fit" values of A and m for each profile and for groups of profiles.

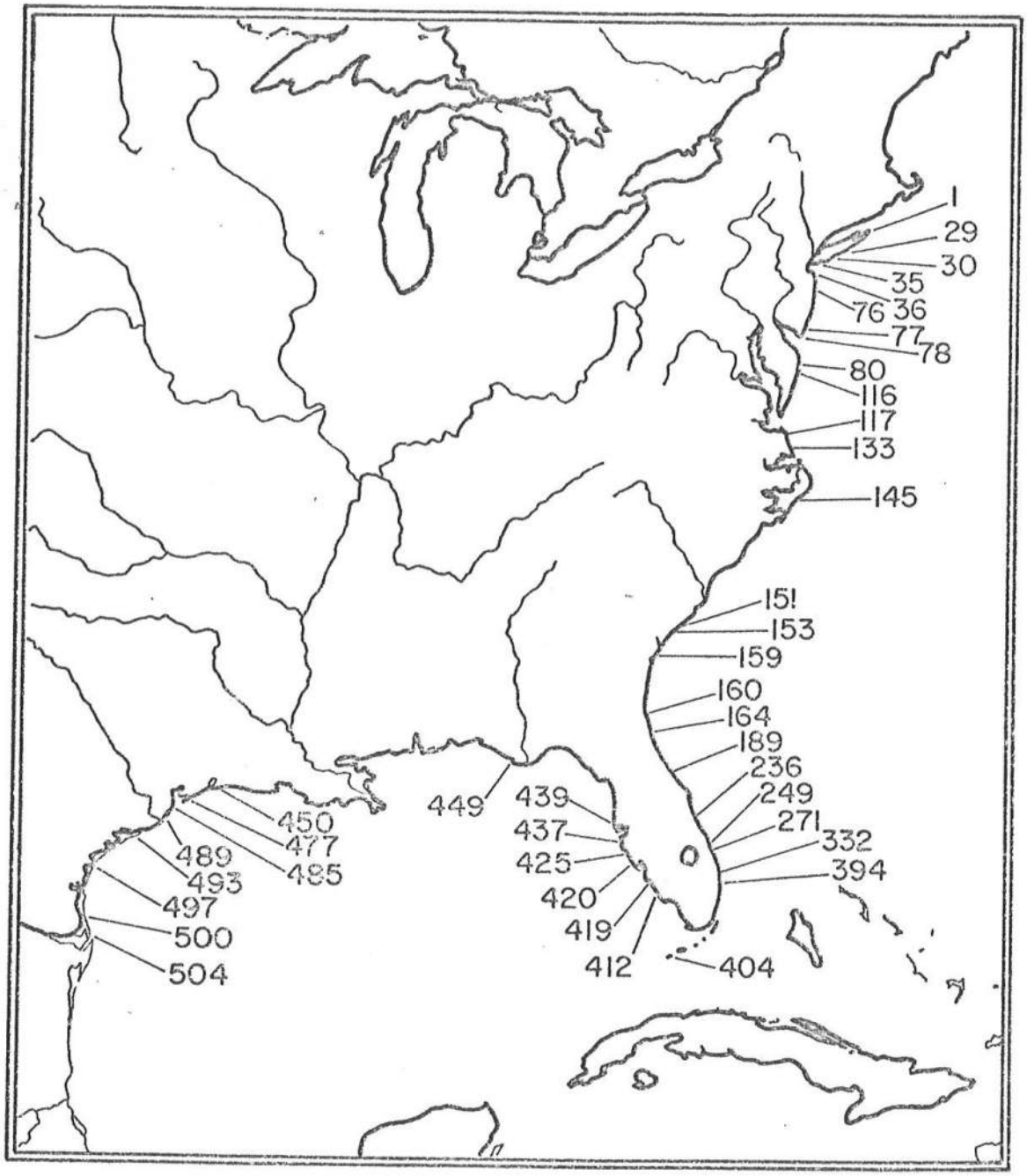

FIGURE 2 Location Map of the 502 Profiles Used in the Analysis (From Hayden, et al.)

METHODOLOGY

"Best fit" values of the parameters A and m were determined by the least squares procedure. Denoting the measured and predicted water depths as $h_{m_{i,n}}$, and $h_{p_{i,n}}$, for each seaward distance $x_{i,n}$ from the surf zone, the predicted depth is

$$h_{p_{i,n}} \equiv A_n \, x_{i,n}^{m_n} \tag{5}$$

in which the subscripts n and i denote the nth profile and distance index across the profile, respectively.

Taking logarithms of both sides,

$$\ell n \; h_{p_{i,n}} = \ell n \; A_n + m_n \; \ell n \; x_{i,n} \tag{6}$$

For the measured data, $h_{m_{i,n}}$ and $x_{i,n}$, the following operation was carried out

$$\underset{\ell n (A_n),\, m_n}{\text{Min}} \; \sum_{i=1}^{I} \left[\ell n \; h_{p_{i,n}} - \ell n \; h_{m_{i,n}} \right]^2 \tag{7}$$

which, by the usual method of least squares, results in the two following equations

$$m_n = \frac{S_{1,n} \, S_{4,n} - I \, S_{3,n}}{(S_{1,n})^2 - I \, S_{2,n}} \tag{8}$$

$$A_n = e^{V_n} \tag{9}$$

where

$$V_n = \frac{S_{1,n}\, S_{3,n} - S_{2,n}\, S_{4,n}}{S_{1,n}^{\,2} - I\, S_{2,n}} \tag{10}$$

and

$$S_{1,n} \equiv \sum_{i=1}^{I} \ell n\, x_{i,n} \quad , \quad S_{2,n} \equiv \sum_{i=1}^{I} (\ell n\, x_{i,n})^2 \tag{11}$$

$$S_{3,n} \equiv \sum_{i=1}^{I} (\ell n\, x_{i,n})(\ell n\, h_{m_{i,n}}), \; S_{4,n} \equiv \sum_{i=1}^{I} (\ell n\, h_{m_{i,n}}) \tag{12}$$

With the values of A_n and m_n determined for each profile, the theoretical profile was calculated from Eq. (4) and the root-mean-square error determined for each profile

$$\varepsilon_n \equiv \sqrt{\frac{1}{I} \sum_{i=1}^{I} (h_{m_{i,n}} - h_{p_{i,n}})^2} \tag{13}$$

A percentage value indicating the error relative to the root-mean-square depth is defined as

$$\delta_n \equiv \frac{\varepsilon_n}{\sqrt{\frac{1}{I} \sum_{i=1}^{I} h_{m_{i,n}}^2}} \times 100\% \tag{14}$$

In addition to the profile parameters, A_n, m_n, ε_n and δ_n, the average of several groups of profiles were calculated and the "best-fit" A and m parameters determined. Finally, for reasons to be presented later, the best least-squares A parameters were determined for each profile with fixed m(= 0.67). Results are described in the next section.

RESULTS

It was of interest to evaluate the characteristics of individual beach profiles and also profiles which may be composed of common sand characteristics and exposed to very nearly the same wave climate. The results presented in this section include the A and m parameters in Eq. (3) and also a measure of goodness-of-fit [Eqs. (13) and (14)] for the profiles.

Individual Profile Results

The least squares procedure was applied to each of the 502 profiles to determine the individual m and A values for each profile. The results are presented for m and A in histogram form in Figures 3 and 4, respectively. It is noted that the dimensions of A are length (ft) to some exponent which is 1-m and, therefore, varies from profile to profile. Figure 3 indicates that there is a range of exponents m which characterize the profiles; however, the mode of the histogram is between 0.6 and 0.7 which is in close agreement with the value of 0.67, found by Bruun (3) and Dean (5) based on different considerations. The value of m = 0.4, which is based on either uniform longshore shear stress distribution or uniform energy dissipation per unit area, occurs much less frequently. The average value of m for all 502 profiles is 0.66. The histogram of the A values for all 502 profiles as presented in Figure 4 shows that the A values range from 0.0025 to 6.31 and that the most commonly occurring value is between 0.0 and 0.30. The average value based on all profiles is 0.362.

Goodness-of-fit parameters were determined for each profile. These parameters are expressed as root-mean-square (rms) errors in Eqs. (13) and (14). The histogram of rms error, ε, is presented as Figure 5. Using the best-fit

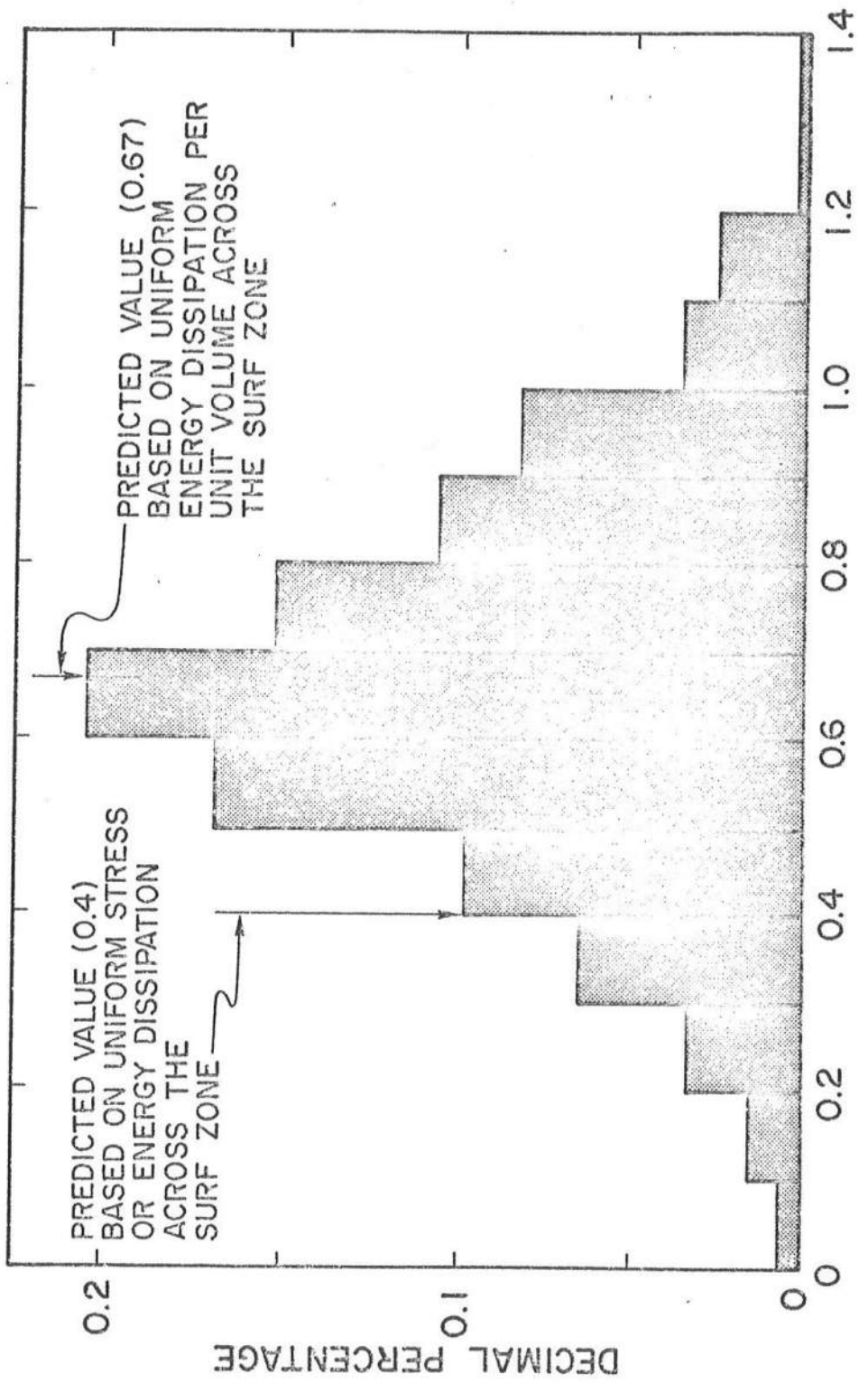

FIGURE 3 Histogram of Exponent m in Equation $h = Ax^m$ for 502 United States East Coast and Gulf of Mexico Profiles

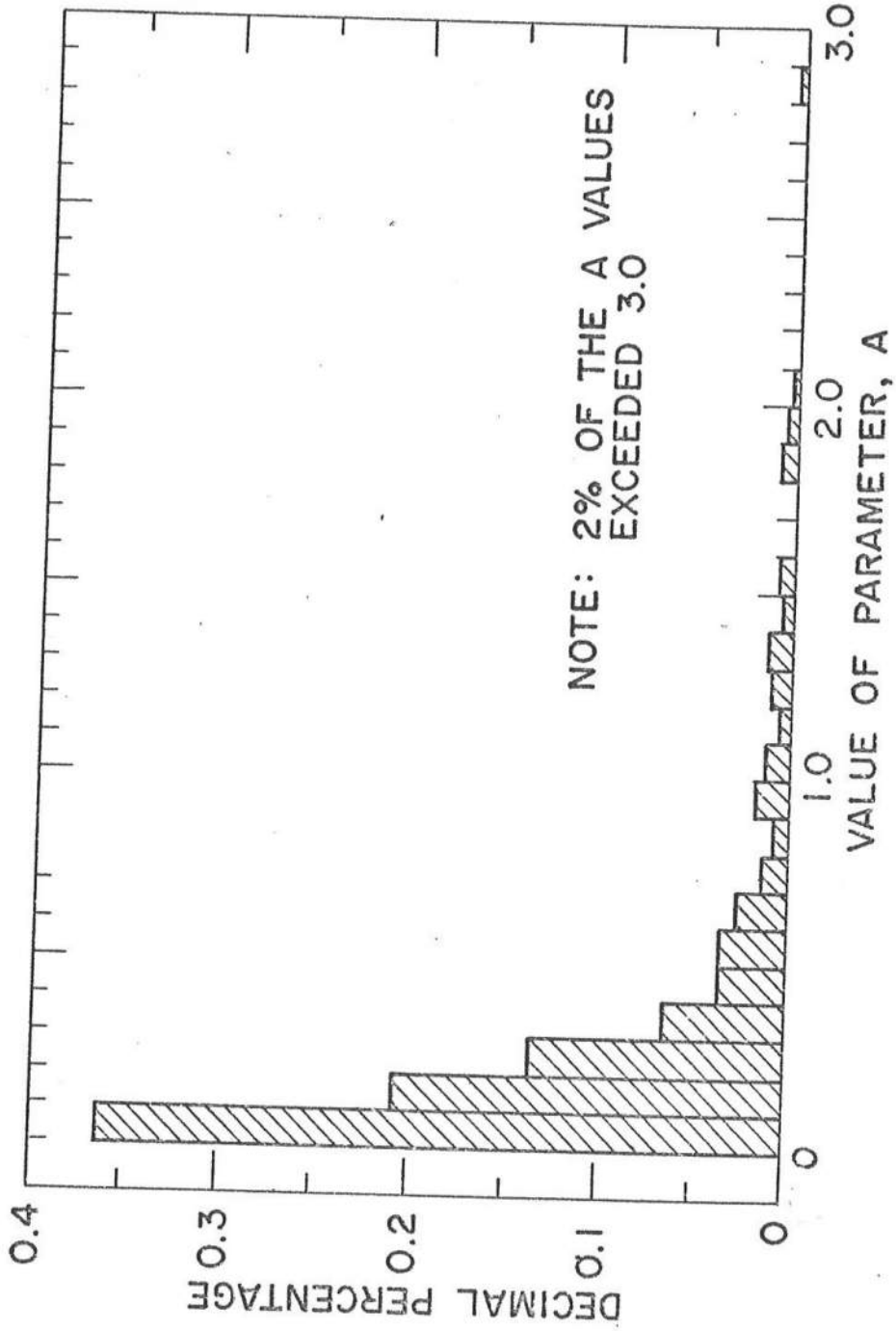

FIGURE 4 HISTOGRAM OF PARAMETER A IN EQUATION $h = Ax^m$ FOR 502 UNITED STATES EAST COAST AND GULF OF MEXICO PROFILES

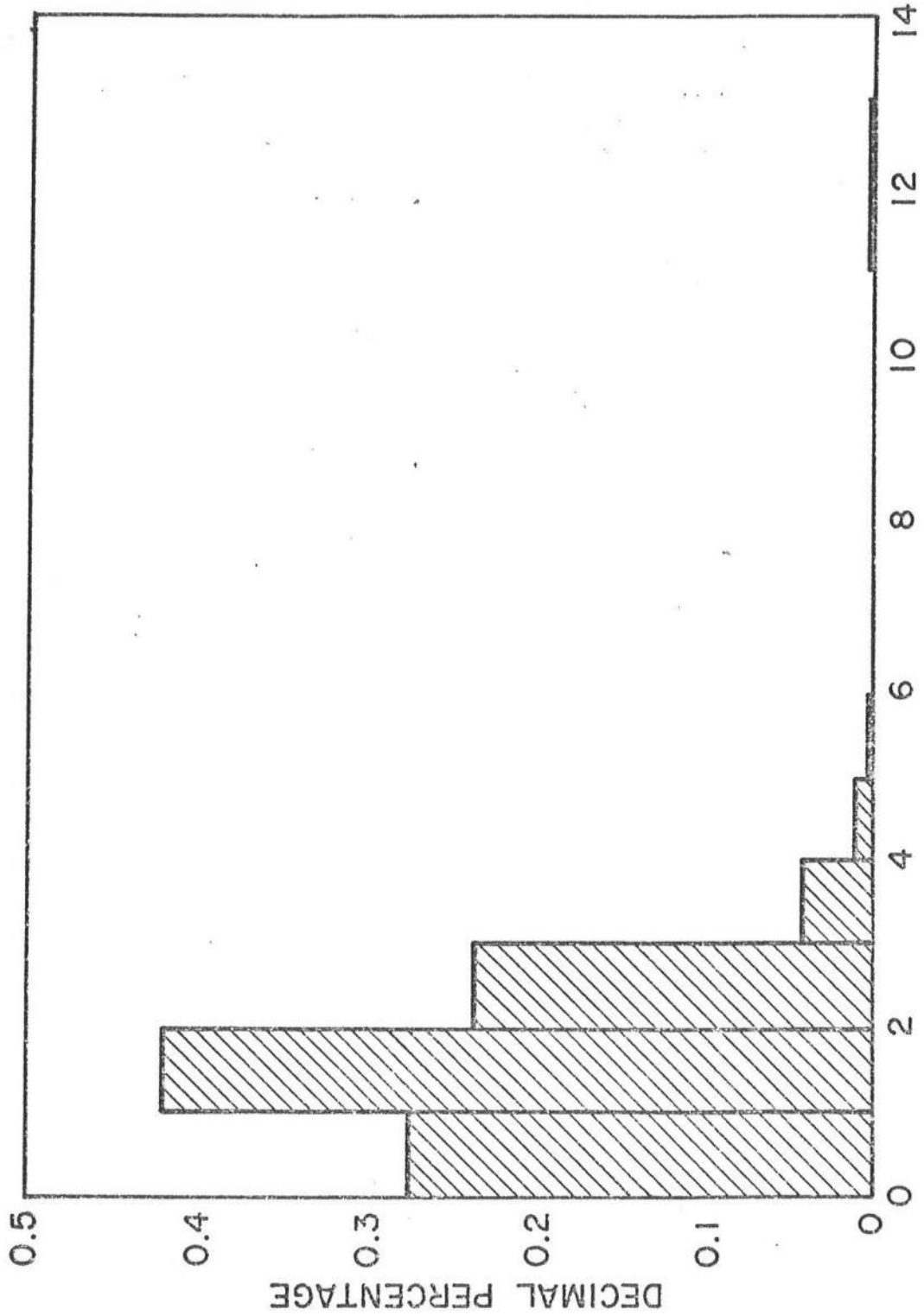

Figure 5 Histogram of Root-Mean-Square Errors Between Fitted and Measured Profiles. All 502 United States East Coast and Gulf of Mexico Profiles.

A and m values determined for each profile a rms profile error of 2.02 ft (0.62 m) and an average percentage error of 16.2% were obtained.

Groups of Profiles

The profiles were grouped into ten data sets according to plausible geomorphic provinces. The profiles included in each data group are presented in Table II. For the analysis, the best-fit m and A values and goodness-of-fit measures were determined for each profile and for the average profile in the data group. The results for the average profile in each data group are presented in Table II and discussed below.

Exponent m--Inspection of the values of the exponents m for the average profiles of each of the various data groups indicates a range 0.52 to 0.82 which is surprisingly small. Although the data may not justify interpretation of a geographical trend, it does appear that there is an initial low value on Long Island, then a rather higher value which extends to Ocracoke Inlet, North Carolina and a lower than average value extending around Florida and to the Brazos Santiago, Texas. There is a general increasing trend in m values for the last few data groups.

Scale Parameter A--The values of the scale parameter, A, range from 0.079 to 0.398 for the ten data groups. There is a correlation between the exponent m and the parameter A for the various data groups, see Figure 6 for a plot of the A, m pairs. This type of feature is not uncommon when two parameters are being fit to data by the least squares (or other) procedure. In our case of beach profiles, the interpretation is simply that a depth at a given distance

TABLE II

CHARACTERISTICS OF BEACH PROFILE DATA GROUPS

Data Group	Profiles	Location *		Characteristics of Data Group			
		From	To	ε (ft) (All Profiles)	Average Profile		
					A	M	ε (ft)
I	1 - 35	Montauk Point N.Y.	Rockaway Beach N.Y.	2.39	0.398	0.533	1.42
II	36 - 78	Sandy Hook N.J.	Cape May N.J.	2.74	0.0793	0.822	1.18
III	79 - 116	Fenwick Light Del.	Ocean City Inlet Md.	2.13	0.0945	0.762	1.54
IV	117 - 145	Virginia Beach Va.	Ocracoke, N.C.	2.18	0.128	0.709	1.54
V	145 - 159	Folly Beach S.C.	Tybee Island Ga.	1.19	0.243	0.523	0.73
VI	160 - 394	Nassau Sound Fla.	Golden Beach Fla.	1.89	0.255	0.594	0.36
VII	395 - 404	Key West Fla.	Key West Fla.	1.33	0.155	0.520	0.76
VIII	405 - 439	Caxambas Pass Fla.	Clearwater Beach Fla.	2.90	0.277	0.554	1.05
IX	440 - 477	St. Andrew Pt. Fla.	Rollover Fish Pass TX	1 .02	0.113	0.644	0.43
X	478 - 504	Galveston TX	Brazos Santiago TX	0.73	0.138	0.620	0.17

* See Figure 2 for Location of the Profiles.

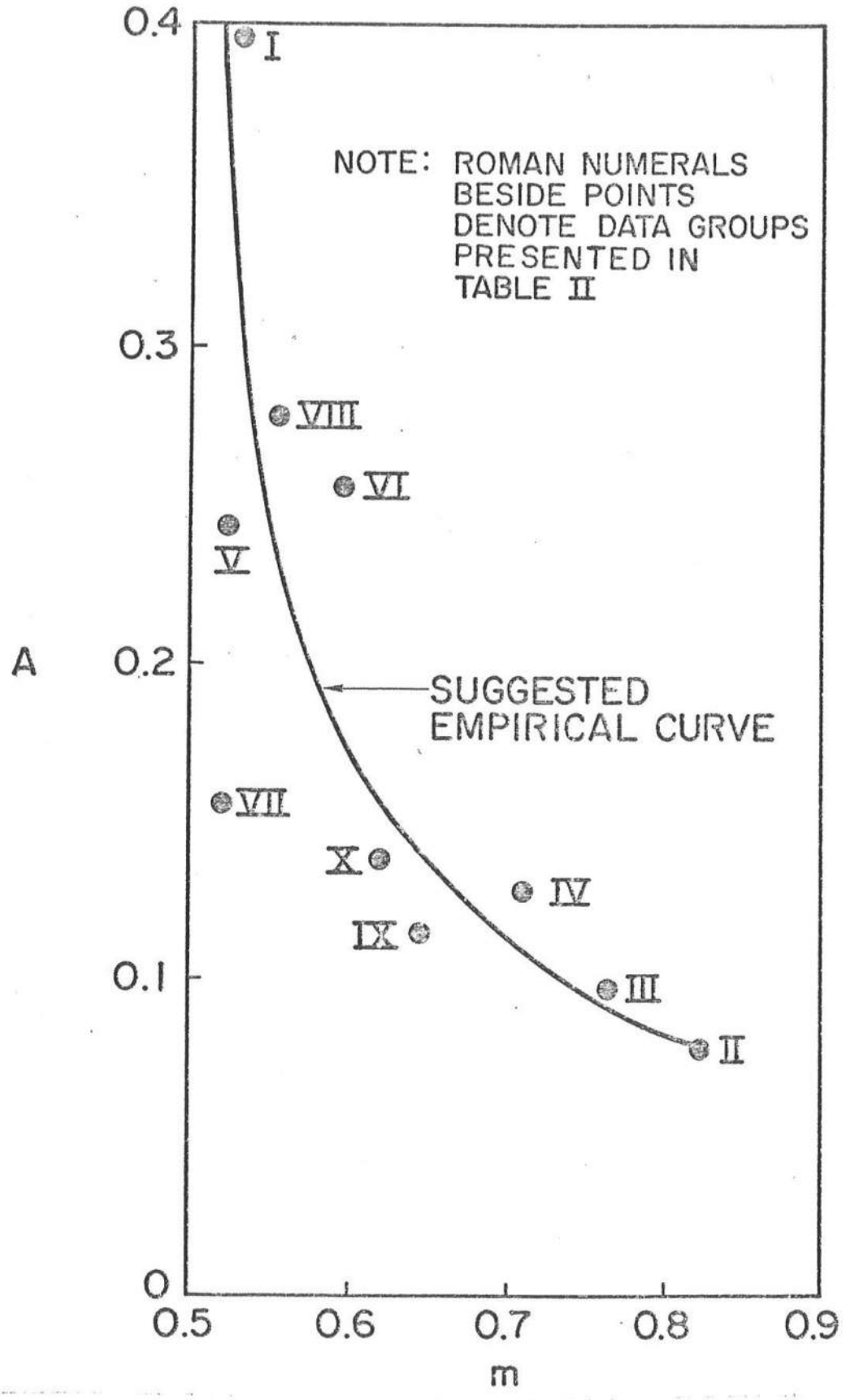

FIGURE 6 Empirical Correlation Between m and A in the Equation $h = Ax^m$. The Data Groups are Shown in Table II and Figure 2.

from shore which can be represented by a particular pair of values of A and m can also be approximately represented by a pair of values of larger A and smaller m or vice versa. Hence the inverse relationship between A and m presented in Figure 6. Stated differently, when considering an entire profile consisting of a number of data points, then due to the inability of the form of the equation to fit all depths exactly, an error which does not differ greatly from the minimum can be associated with a number of pairs of the parameters. In summary, it is doubtful whether any physical significance should be attributed to the relationship presented in Figure 6.

Goodness-of-Fit Parameter--The percentage goodness-of-fit parameters for the average profiles of the various data groups range from 2.1% to 15.5%. Expressed in dimensional terms, this corresponds to a root-mean-square deviation between the average profile and the best-fit to that profile of 0.17 ft (0.05 m) to 1.54 ft (0.47 m), which appears to be reasonably good.

General Features of Beach Profiles--In order to provide a visual indication of the various average profiles of the data groups and the best fit equations, a number of plots of beach profiles were prepared.

As an example of a particular data group, Figure 7 presents, for Data Group I, the average beach profile, the maximum and minimum depths at 50 ft (15.2 m) spacings offshore and the best-fit equation of the form of Eq. (3). The root-mean-square error for each location along the profiles is shown in Figure 8.

It is interesting to examine the general shape characteristics of the average profiles and their best-fit representations of the form of Eq. (3).

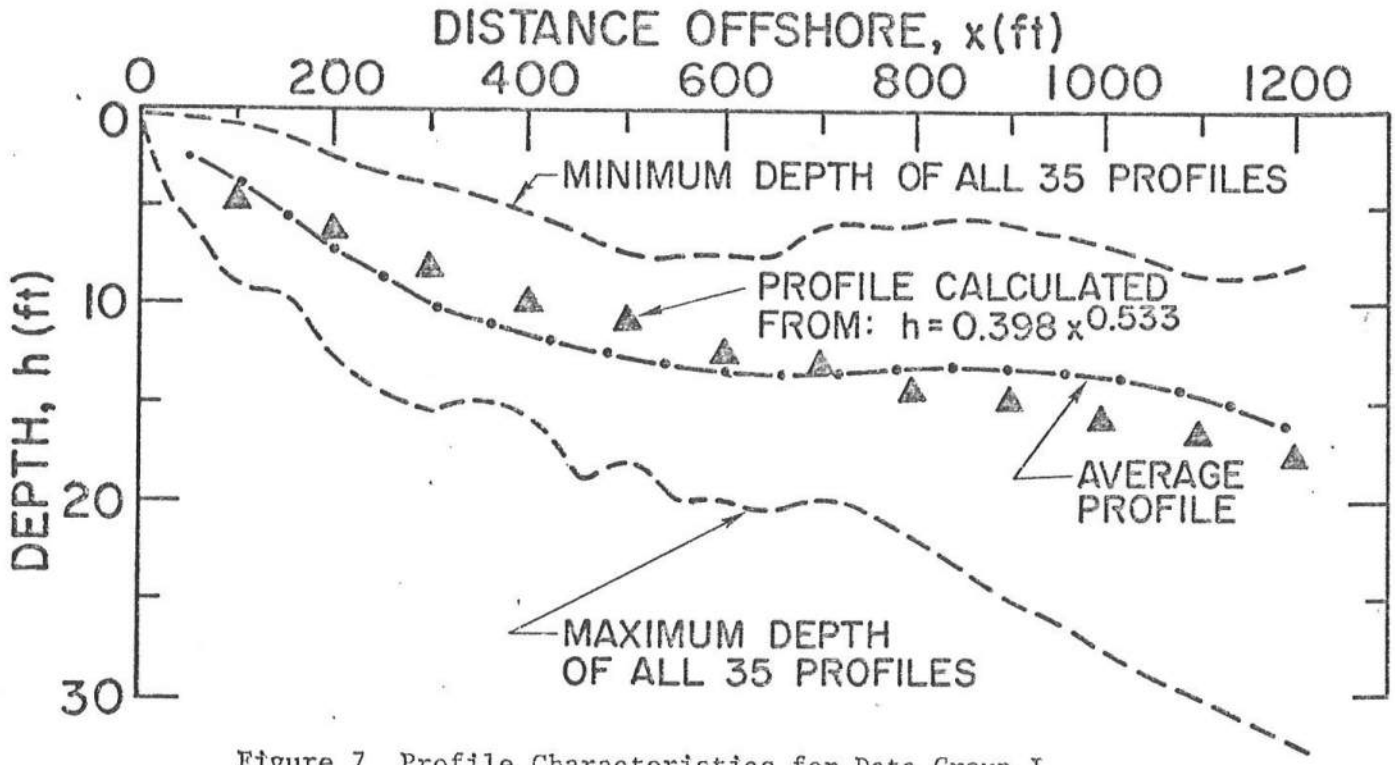

Figure 7 Profile Characteristics for Data Group I

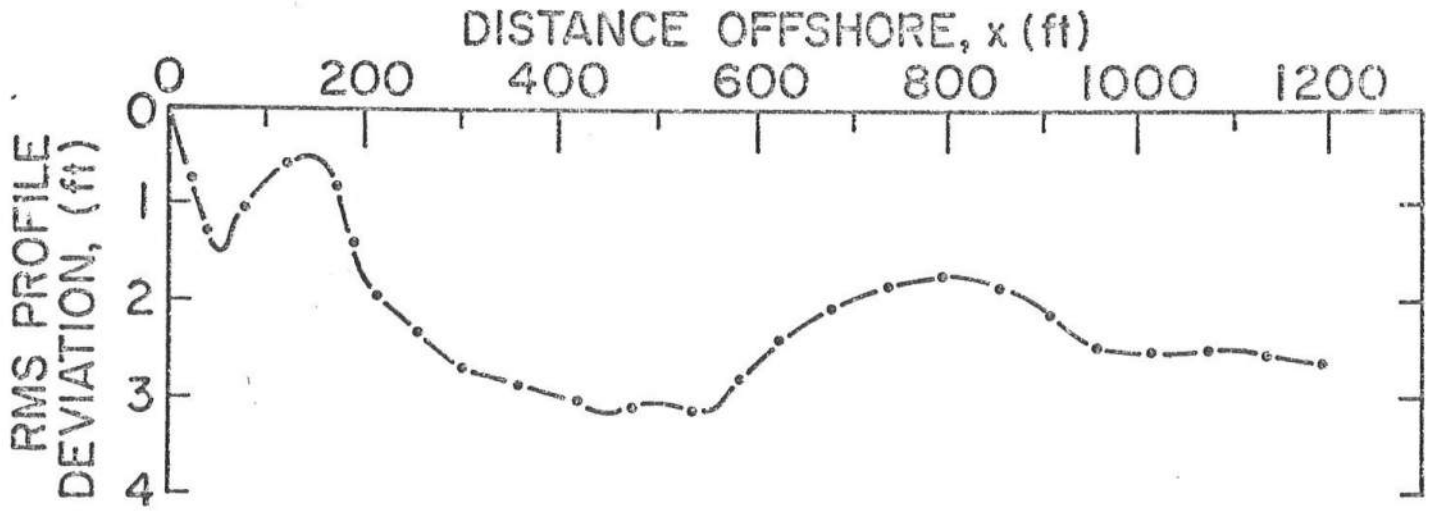

FIGURE 8 Root-Mean-Square Deviation Between Individual Measured and Fitted Profiles Versus Distance Offshore. Data Group I

Figures 9 and 10 present, for each of the 10 data groups, the average measured profiles, the best fit to those profiles and, for reference purposes, the average of all 502 profiles.

Individual Profile Results, m Fixed at 0.67

Based on the results presented heretofore, it appears realistic to fix the exponent m at 0.67 and, considering A as the only free variable (Eq. 3), determine the fit to the individual profiles. The least squares procedure used is not detailed here as it is straightforward. The histogram of the A parameters is presented as Figure 11. The overall root-mean-square profile error as defined in Eq. (13) was 2.13 ft (0.65 m) as compared to 2.02 ft (0.62 m) for the case of allowing m and A as free variables. This small difference in errors supports the earlier argument that m can be considered to be a constant (m = 0.67) and that the parameter A is a function of sediment (and possibly wave) characteristics. An advantage of utilizing m = 0.67 is that the dimensions of A_3 are $(\text{length})^{1/3}$ and, as shown in Appendix III, A_3 has the form

$$A_3 = \left[\frac{24}{5}\frac{\mathcal{D}_3(D)}{\gamma\sqrt{g}\ \kappa^2}\right]^{2/3} \tag{15}$$

in which $\mathcal{D}_3(D)$ represents an energy dissipation rate per unit volume under which a sediment particle of size D is stable. In actuality, $\mathcal{D}_3$ should also depend on shape and specific gravity.

Appendix IV shows that with certain assumptions the functional dependence of $\mathcal{D}_3$ is best expressed in terms of fall velocity, w as

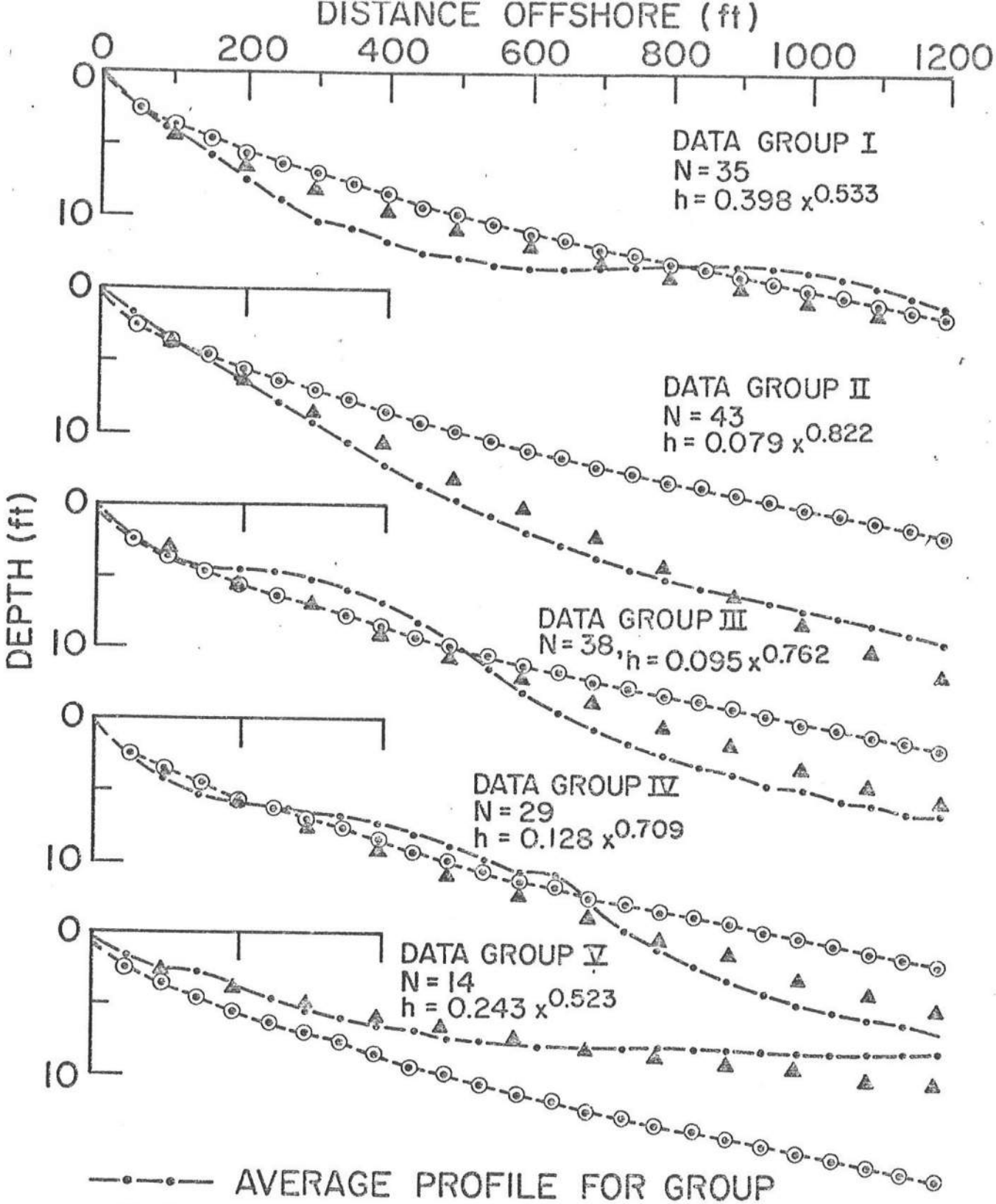

FIGURE 9 Comparison of Beach Profiles for Data Groups I-V.

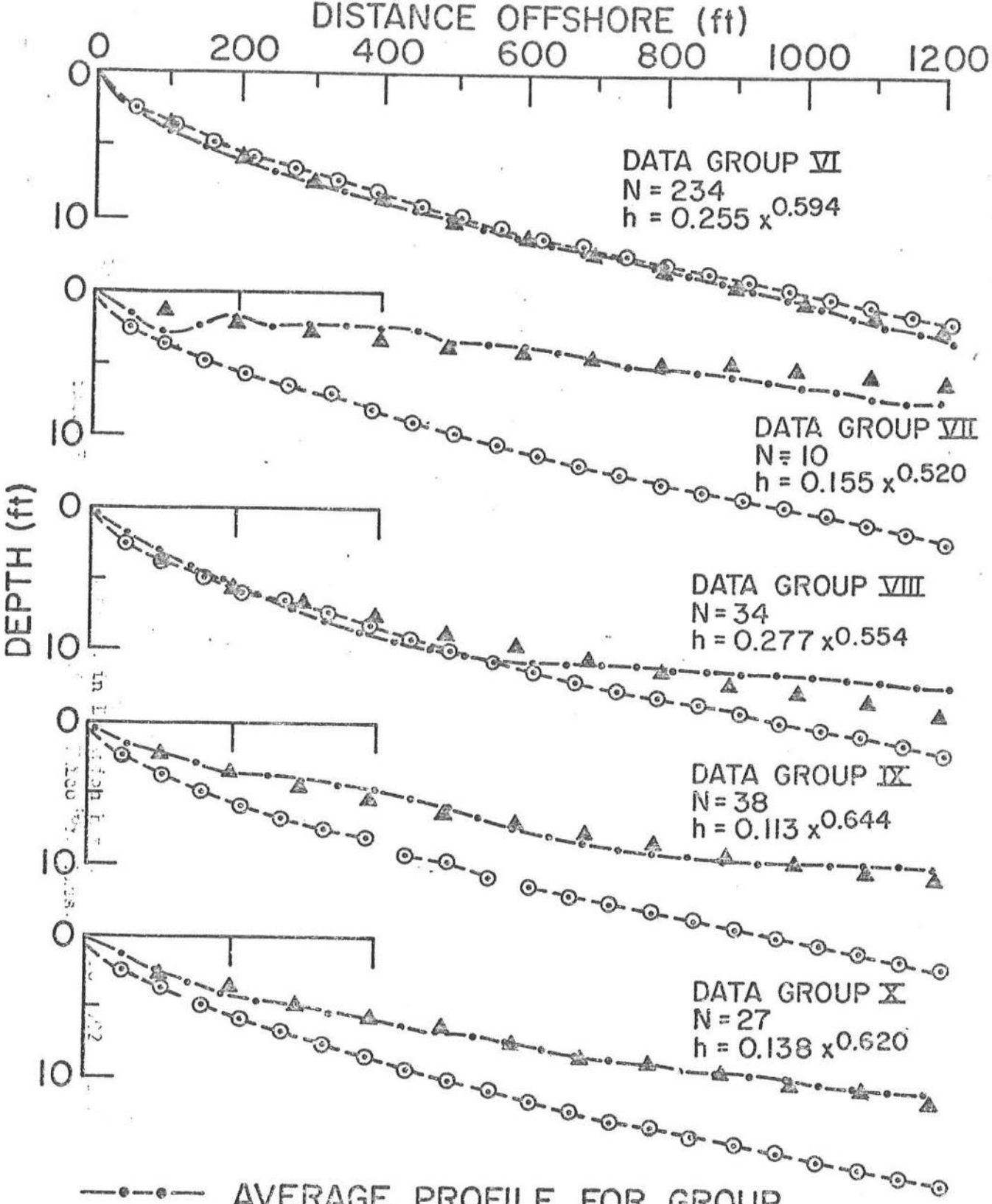

FIGURE 10 Comparison of Beach Profiles for Data Groups VI-X.

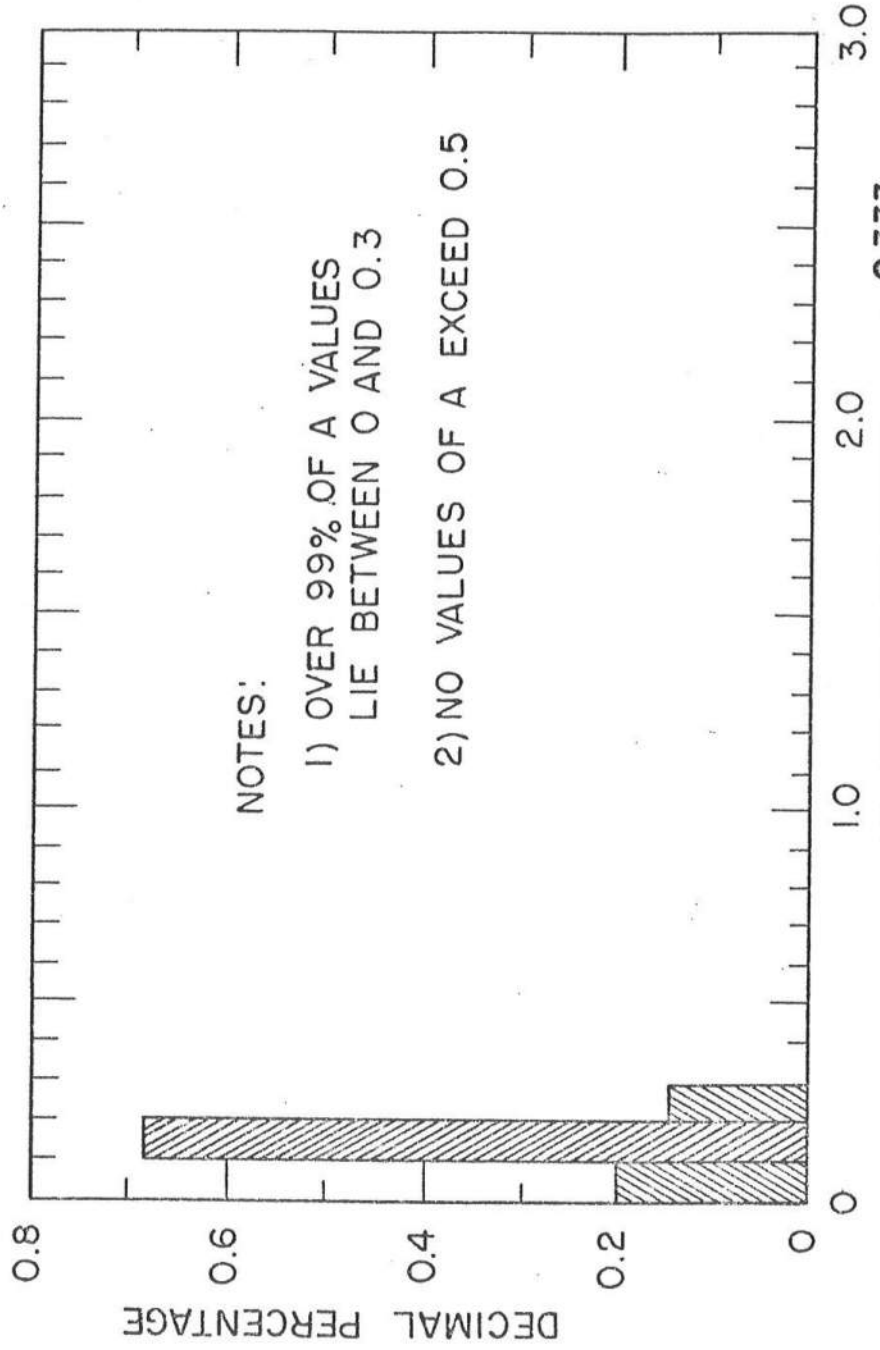

FIGURE 11 Histogram of Parameter A in Equation $h = A\,x^{0.67}$ for 502 United States East Coast and Gulf of Mexico Profiles.

$$\mathcal{D}_3 \propto w^2 \tag{16}$$

or for a Reynolds number range in which the quadratic drag law applies

$$\mathcal{D}_3 \propto D \tag{17}$$

Based on the considerations of Appendix IV and the data presented in this paper the relationship of $\mathcal{D}_3$ with particle diameter, D, for water temperatures of 10°, 20° and 30°C is presented in Figure 12.

EXAMPLE OF BEACH PROFILE COMPUTATIONS

As an example of the computation of equilibrium beach profiles by the method presented here, consider two profiles for which the effective sediment diameters are 0.15 and 0.3 mm and the water temperature is 20°C. The associated values of $\mathcal{D}_3$ and A_3 determined from Figure 12 and Eq. (15), respectively, are presented in Table III and the equilibrium profiles

TABLE III

Parameters of Example Equilibrium Beach Profiles
(Temperature = 20°C)

Sand Diameter (mm)	$\mathcal{D}_3$ (lb - $ft^{-2}sec^{-1}$)	A_3 $(ft)^{1/3}$
0.15	0.42	0.0437
0.30	2.6	0.1473

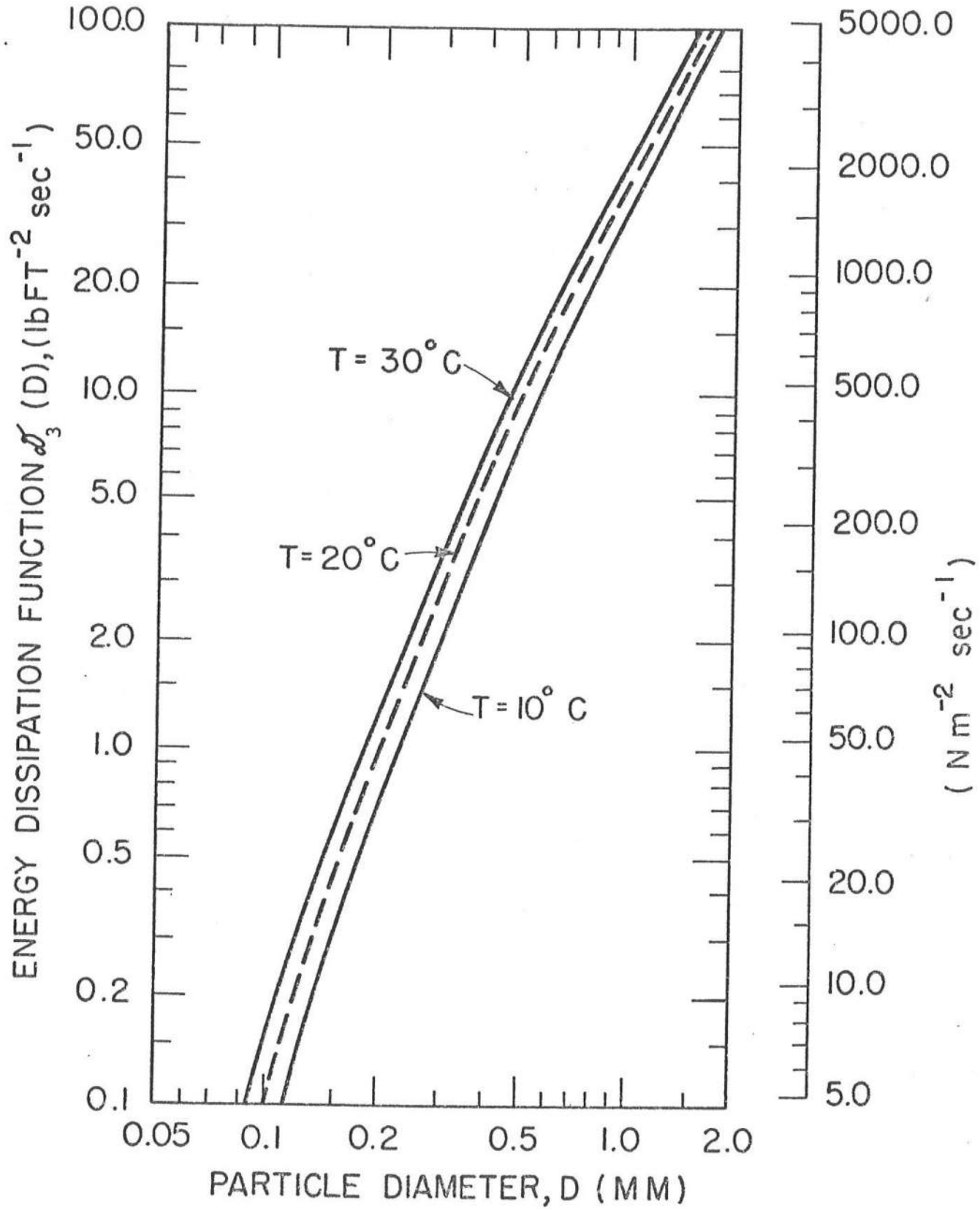

FIGURE 12 Preliminary Relationship Between Dissipation Parameter D_3 and Diameter D for Quartz Spheres

calculated from Eq. (3) are presented in Figure 13. It is noted that the profile associated with the coarser sand is steeper than that with the finer sand, a feature evident from natural profiles.

SUMMARY AND CONCLUSIONS

Operative within the surf zone are "constructive" and "destructive" agents which tend to transport material onshore and offshore, respectively. Based on previous work by Bruun (3) and Dean (5) relating to these destructive agents, the equilibrium beach profile is found to be of the form

$$h = A\, x^m$$

in which h is the water depth at a distance x from shore and A and m are scale and shape parameters, respectively. Depending on the destructive mechanism, m is predicted to be 0.4 and/or 0.67. The parameter A should depend on the stability characteristics of the bottom material. Using 502 beach profiles from the Atlantic and Gulf of Mexico shorelines, the parameters A and m were determined by conducting a least-squares fit to Eq. (3). Although bars are present in some of the profiles, there was reasonably good fit with a root-mean-square error of 2.02 ft (0.62 m). The histogram of m displays a dominant value near 0.67, thereby indicating turbulent water particle fluctuations as the destructive agent. The histogram of individual profile m values is fairly peaked with 53% of the exponents occurring between 0.5 and 0.8. The parameter A was found to vary from 0.0025 to 6.31. The data were grouped into

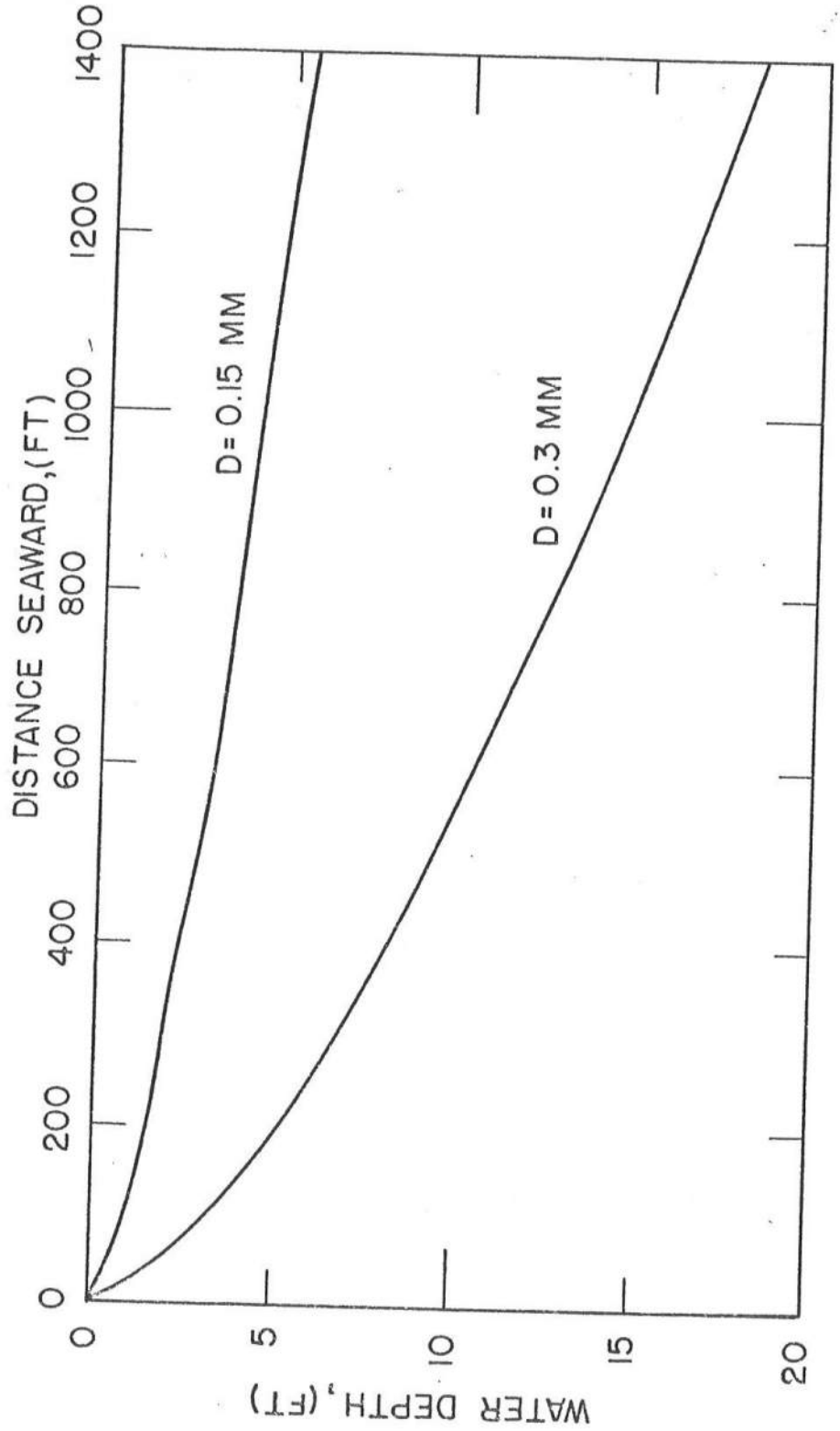

FIGURE 13 Computed Beach Profiles for Sands of Two Different Sizes

ten geomorphic provinces and the parameters A and m determined for the averages of all profiles falling into those groups. It was found that these values of m ranged from 0.52 to 0.82 and the A values ranged from 0.079 to 0.398. The empirical relationship between A and m (Figure 6) suggests a spurious correlation in which pairs of large A and small m or vice versa could fit a given profile reasonably well. Based on the previously mentioned histogram of m values centered approximately at 0.67, a least squares fit to each of the 502 profiles was conducted in which m was fixed at 0.67 and the parameter A was the only free variable. The result was a much reduced range of the parameter A (Compare Figures 4 and 11) and only a slightly increased average rms profile error [2.02 ft (0.62 m) vs. 2.13 ft (0.65 m)]. This strongly supports that fixing m at 0.67 is realistic and that the dominant mechanism governing equilibrium beach profiles is the stability of the sediment under a certain level of turbulent water particle fluctuations. Based on this consideration, a relationship is developed between the wave energy dissipation rate per unit volume and the fall velocity, w, of a sediment particle. This allows calculation of equilibrium beach profiles from the sediment characteristics (fall velocity or size).

Finally, it is noted that a reasonable understanding of the shape characteristics of equilibrium beach profiles should represent the first step in analyzing barred (storm) profiles.

ACKNOWLEDGMENTS

As noted previously, the author is indebted to Dr. John Fisher for providing the beach profiles used in this paper. Partial financial support by the

Department of Civil Engineering and the Sea Grant Program at the University of Delaware are acknowledged.

APPENDIX I REFERENCES

1. Bagnold, R.A., "Motion of Waves in Shallow Water - Interaction Between Waves and Sand Bottoms," Proc. Roy. Soc., Ser. A, V. 187, 1946, p. 1-15.

2. Bowen, A. J., Inman, D.L. and Simmons, V.P., "Wave 'Set-Down' and Wave Set-Up," J. of Geophys. Res., V. 73, No. 8 , 1968, pp. 2569-2577.

3. Bruun, P., "Coast Erosion and the Development of Beach Profiles," Beach Erosion Board, Tech. Memo. No. 44, 1954.

4. Bruun, P., "Sea-Level Rise as a Cause of Shore Erosion," J. Waterways, Harbors and Coastal Engrg. Div., ASCE, V. 88, WW1, Feb., 1962, pp. 117-130.

5. Dean, R. G., "Equilibrium Beach Profiles and Response to Storms," to be published in Proc. 15th Conf. on Coastal Engrg., Honolulu, Hawaii, July, 1976.

6. Eagleson, P.S., Glenne, B., and Dracup, J.A., "Equilibrium Characteristics of Sand Beaches," J. Hydraulics Div., ASCE, V. 89, No. HY1, Jan., 1963, pp. 35-57.

7. Fenneman, N.M., "Development of the Profile of Equilibrium of the Subaqueous Shore Terrace," J. of Geology, V. X, 1902, p. 1-32.

8. Hayden, B., Felder, W., Fisher, J., Resio, D., Vincent, L. and Dolan, R., "Systematic Variations in Inshore Bathymetry," Tech. Rept. No. 10, Dept. of Env. Sciences, Univ. of Virginia, Jan., 1975.

9. Keulegan, G.H. and Krumbein, W.C., "Stable Configuration of Bottom Slope in a Shallow Sea and Its Bearing on Geological Processes," Trans. Amer. Geophys. Union, V. 30, No. 6, 1919, p. 855-861.

10. Longuet-Higgins, M.S., "Longshore Currents Generated by Obliquely Incident Sea Waves," Parts 1 and 2, J. of Geophys. Res., V. 75, No. 33, 1970, pp. 6778-6801.

11. Rector, R.L., "Laboratory Study of Equilibrium Beach Profiles,"Beach Erosion Board, Tech. Memo. No. 41, August, 1954.

12. Saville, T., "Scale Effects in Two-Dimensional Beach Studies," Trans. 7th Meeting, Inter. Assoc. of Hydraulic Res., Lisbon, 1957, pp. A3-1 to A3-9.

13. Watts, G.M. and Dearduff, R.F., "Laboratory Study of Effect of Tidal Action on Wave-Formed Beach Profiles," Beach Erosion Board, Tech. Memo. No. 52, Dec., 1954.

APPENDIX II NOTATION

The following symbols are used in this paper:

A, A'	Scale factors in equilibrium beach profiles developed by Bruun.
A_i	Scale factor in equilibrium beach profile. The subscript i = 1,2,3 applies to equilibrium beach profile models I, II and III, respectively, see Eqs. (3), (24), (25), (28), (29), (31) and (32).
B_i	Factors characterizing shape of sediment particle (i=1,2,3,4)
$\_\__b$	Subscript "b" denoting wave conditions.
C	Wave celerity.
C_G	Group velocity.
D	Sediment particle diameter.
e_t	Turbulent energy density (per unit volume).
E	Wave energy per unit plan area.
F	Hydrodynamic destructive forces on sediment particle (Eq. (35)).
g	Gravitational constant.
h	Water depth.
H	Wave height.
I	Number of depths defining a given profile.
$\_\__i$	Subscript "i" denoting i^{th} location across a profile.
m	Shape factor of equilibrium beach profile.
$\_\__m$	Subscript "m" indicating measured value.
N	Number of profiles comprising a data group
$\_\__n$	Subscript "n" denoting n^{th} profile.
$\_\__p$	Subscript "p" indicating "predicted" value
S_i	Sums as defined in Eqs. (11) and (12), i = 1,2,3,4.

S_{xy} Flux, in the x direction of the y-component of momentum.

t Time.

T Wave period.

u' Turbulent water particle velocity.

u_T Total water particle velocity.

u_w Water particle velocity associated with organized wave motion.

V Convective velocity of turbulent energy transfer.

V_n Parameter related to profile scale factor, A_n, c.f., Eqs. (9) and (10)

w Fall velocity of sediment particle.

W Surf zone width.

W_s Submerged weight of sediment particle.

x Horizontal coordinate oriented perpendicularly outward from shore, origin at shoreline.

x' Horizontal coordinate oriented perpendicularly toward shore, origin at surf line.

y Horizontal coordinate oriented parallel to shore.

$\mathcal{D}_i$ Wave energy dissipation rate which can be sustained by sediment particles, i = 2,3 for equilibrium beach profiles II and III, respectively.

α Angle between wave crest and bottom contours.

β Transfer rate of turbulent energy to heat.

γ Specific weight of water.

δ_n Percentage error for n^{th} profile as defined by Eq. (14).

ε_n Root-mean-square error for n^{th} profile as defined by Eq. (13).

κ Ratio of spilling breaker height to depth.

τ Longshore component of bottom shear stress.

ρ Mass density of water.

ρ_s Mass density of sediment particle.

APPENDIX III DERIVATION OF EQUILIBRIUM BEACH PROFILES

Introduction

In this appendix the forms of three equilibrium beach profiles will be developed. Linear wave theory will be employed and the ratio of breaking wave height to water depth will be taken as a constant landward of the point of first wave break. The results are, therefore, strictly applicable only to spilling breakers.

Model I. Beach Profile Due to Uniform Alongshore Shear Stress

Consider waves arriving obliquely to the shore as shown in Figure 14. It is well known (3)(10) that there is a flux of momentum due to the wave motion and that this flux of momentum is representable as a tensor which is proportional to the square of the wave height. As the waves break and propagate through the surf zone, the wave height is reduced and this necessitates a transfer of momentum from the organized waves to the water columns within the surf zone. For the case of straight and parallel bottom contours which we shall consider here, the flux in the onshore direction of the onshore component of momentum is balanced by a "set-up" within the surf zone. The flux in the onshore direction of the longshore component of momentum, S_{xy}, results in a transfer of longshore momentum to the water columns and distributed longshore shear stress on the bottom, which, if there is no wave reflection, must integrate exactly to S_{xy} evaluated at the surf line. The actual distribution of the longshore component of bottom shear

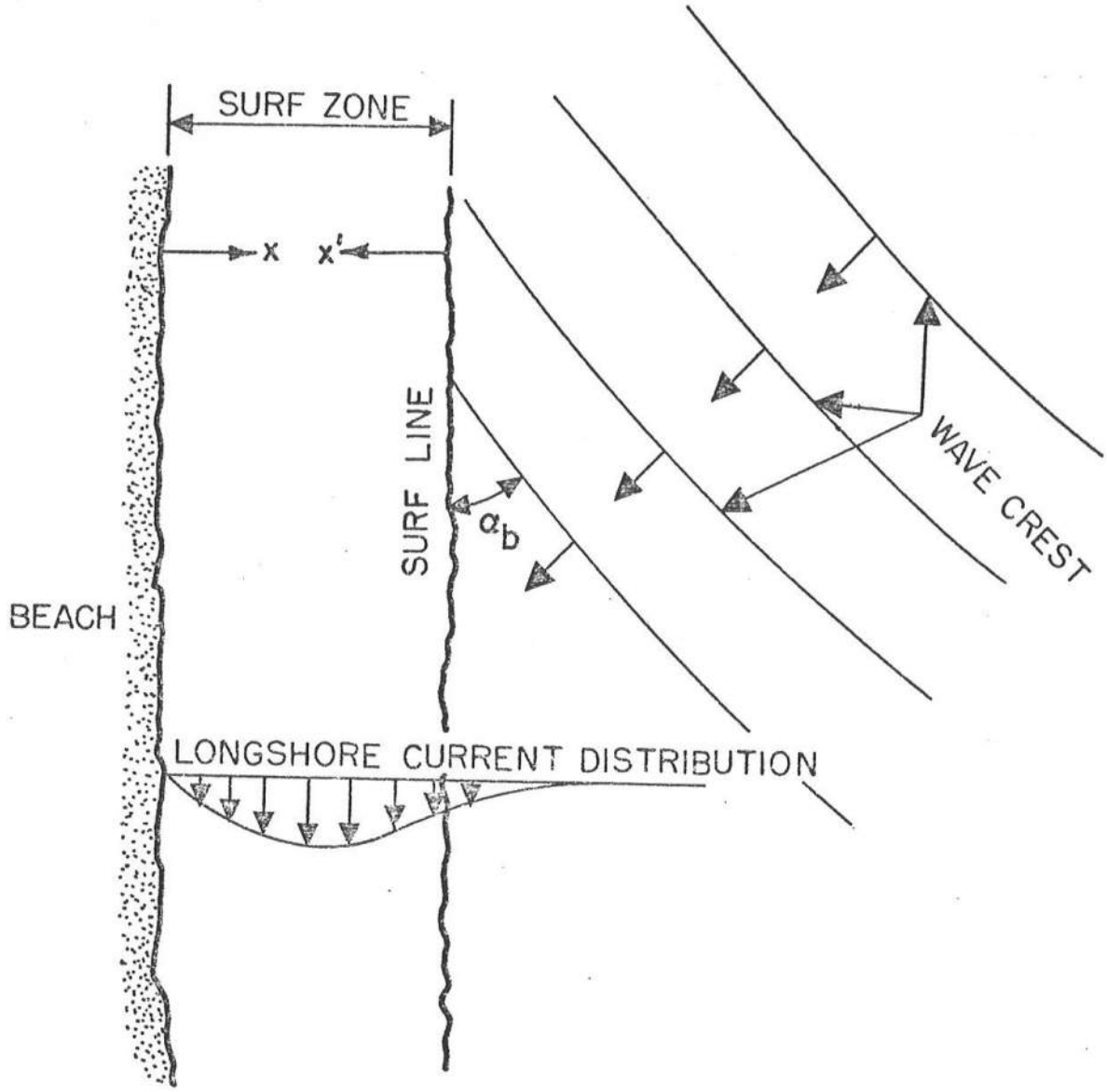

FIGURE 14 Definition Sketch for Waves Approaching Obliquely to Shoreline

stress, τ, is affected by the transfer of momentum from adjacent water columns; however, for purposes here, it will be assumed that there is no lateral shear coupling between adjacent water columns. The local longshore component of shear stress on the bottom is, therefore, the value transferred due to local breaking and is

$$\tau(x) = - \frac{\partial S_{x'y}}{\partial x'} \tag{18}$$

where x and x' are horizontal coordinates directed offshore and onshore, respectively and it can be shown that $S_{x'y}$ the flux of the y-component of momentum in the x'-direction for shallow water conditions, is

$$S_{x'y} = \gamma \frac{H^2}{8} \sin \alpha \cos \alpha \tag{19}$$

where linear shallow water wave theory has been utilized. Considering spilling breaking waves, idealized bathymetry with bottom contours straight and parallel and Snell's Law for refraction, the following apply

$$H = \kappa h \tag{20}$$

$$C = \sqrt{gh} \tag{21}$$

$$\frac{\sin \alpha}{C} = \text{constant} \tag{22}$$

where κ can be represented approximately as a constant ($\simeq 0.8$). Carrying out the differentiation indicated by Eq. (18), approximating cos α by unity, and replacing -dx' by dx, the alongshore component of bottom shear stress is

$$\tau = \frac{5}{16} \gamma \kappa^2 \sqrt{g} \frac{\sin \alpha}{C} h^{3/2} \frac{dh}{dx} \tag{23}$$

and if the longshore shear stress which can be sustained by a sediment particle of diameter D is $\tau(D)$, then integration of Eq. (23) yields

$$h = A_1 x^{0.4} \tag{24}$$

in which

$$A_1 = \left(\frac{8}{\gamma \kappa^2} \frac{\tau(D)}{\sqrt{g}} \frac{C}{\sin \alpha}\right)^{0.4} \tag{25}$$

Model II - Beach Profile Due to Uniform Energy Dissipation Per Unit Surface Area

In this model, it is considered that the energy dissipation per unit surface area is uniform across the surf zone. The energy dissipated is first transferred into turbulence, then, through viscous action, into heat.

The energy flux within the surf zone can be expressed by

$$\frac{\partial E}{\partial t} + \frac{\partial (EC_G)}{\partial x'} = -\mathcal{D}_2(D) \tag{26}$$

in which C_G represents the group velocity, and $\mathcal{D}_2$ is the rate at which energy is dissipated per unit area. In the preceding equation, it is considered that a sand of a certain size, D, (or more generally stability characteristics including shape and specific gravity) can withstand a certain rate of energy

dissipation per unit area in the overlying water column. The parameter $\mathcal{D}_2$ then becomes a characteristic of the particle size, D, i.e., $\mathcal{D}_2(D)$. Considering steady conditions when averaging over a wave period and utilizing the same small amplitude shallow water wave relationship, as in Model I, it is found that

$$\frac{\partial (EC_G)}{\partial x} = \frac{\gamma}{8} \sqrt{g}\, \kappa^2 \frac{\partial}{\partial x} h^{5/2} = \mathcal{D}_2(D) \tag{27}$$

or
$$h = A_2\, x^{0.4} \tag{28}$$

in which
$$A_2 = \left[\frac{8\, \mathcal{D}_2(D)}{\gamma \sqrt{g}\, \kappa^2}\right]^{0.4} \tag{29}$$

It is noted that the more stable the sand, the larger A_2 and hence, the steeper the profile.

Model III - Beach Profile Due to Uniform Energy Dissipation Per Unit Volume

This model is very similar to Model II, except that the consideration is now made that a particle with given stability characteristics can withstand a certain rate of wave energy dissipation per unit volume, $\mathcal{D}_3(D)$ without remolding of the bottom to a more stable slope. This consideration yields

$$\frac{\partial (EC_G)}{\partial x} = \frac{\gamma}{8} \sqrt{g}\, \kappa^2 \frac{\partial}{\partial x} (h^{5/2}) = h\, \mathcal{D}_3(D) \tag{30}$$

Carrying out the operations indicated by Eq. (30),

$$h = A_3 x^{2/3} \tag{31}$$

in which

$$A_3 = \left[\frac{24}{5} \frac{\mathcal{D}_3}{\gamma\sqrt{g}} \frac{(D)}{\kappa^2}\right]^{2/3} \tag{32}$$

APPENDIX IV VARIATION OF DISSIPATION FACTOR, $\mathcal{D}_3$, WITH SEDIMENT CHARACTERISTICS

There are several possible relationships which could be proposed to represent the variation of the dissipation factor $\mathcal{D}_3$ with sediment characteristics (c.f., Eq. 30).

Since the results of the analysis presented herein indicate strongly that energy dissipation rate per unit water volume governs the form of natural beach profiles, it is instructive to consider qualitatively the process of energy dissipation in the surf zone. For realistic (nonlinear) breaking waves the energy is clearly concentrated in the crest region. An impulsive rate of transfer from organized wave energy to turbulent fluctuations as shown in Figure 15-a would represent an idealization of this process. The intensity of turbulent fluctuations in the surf zone is regarded as the destructive agent affecting the stability of the sediment particles; it, therefore, would be necessary to solve the following equation to examine the problem quantitatively

$$\frac{\partial e_t}{\partial t} + \frac{\partial}{\partial x}(V\, e_t) = \mathcal{D}_3 - \beta(t) \qquad (33)$$

in which e_t represents the turbulent energy density per unit volume, V is the convective velocity of turbulent energy transfer and β the transfer rate from turbulent energy to heat. The term $\mathcal{D}_3$ represents the production of turbulent energy via the dissipation of organized wave energy. Although

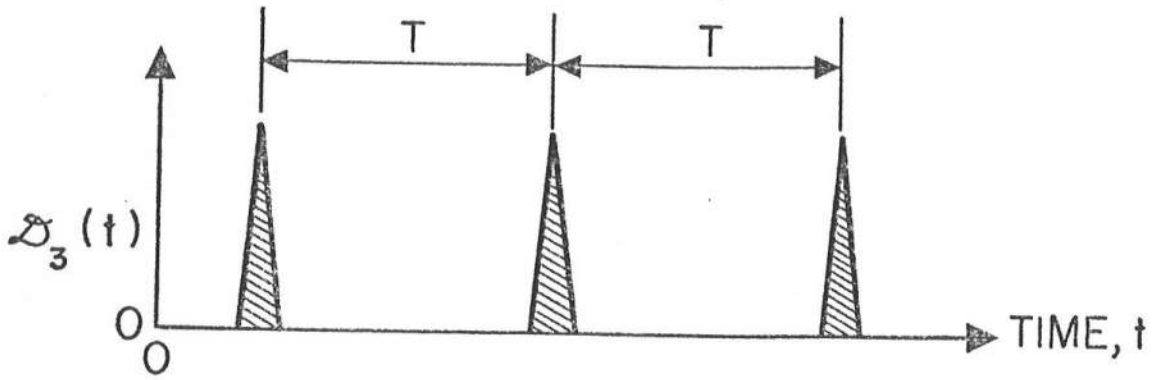

A) IDEALIZED IMPULSIVE RATE OF TURBULENT ENERGY PRODUCTION PER UNIT VOLUME $\mathcal{D}_3(t)$

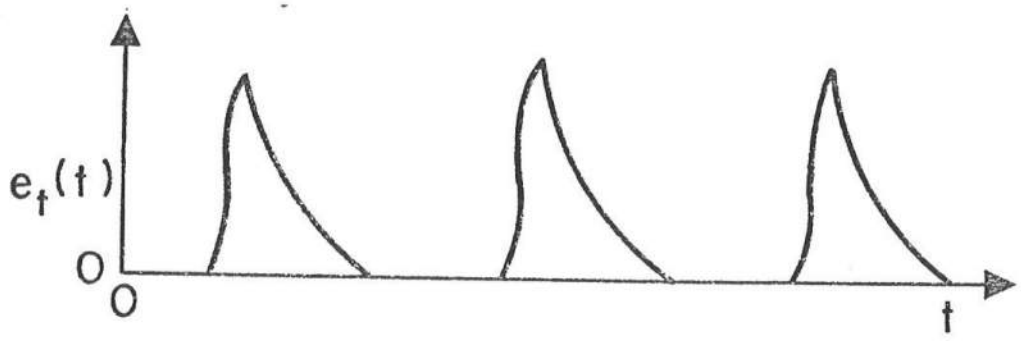

B) TURBULENCE ENERGY DENSITY, $e_t(t)$ FOR LARGE DECAY, β

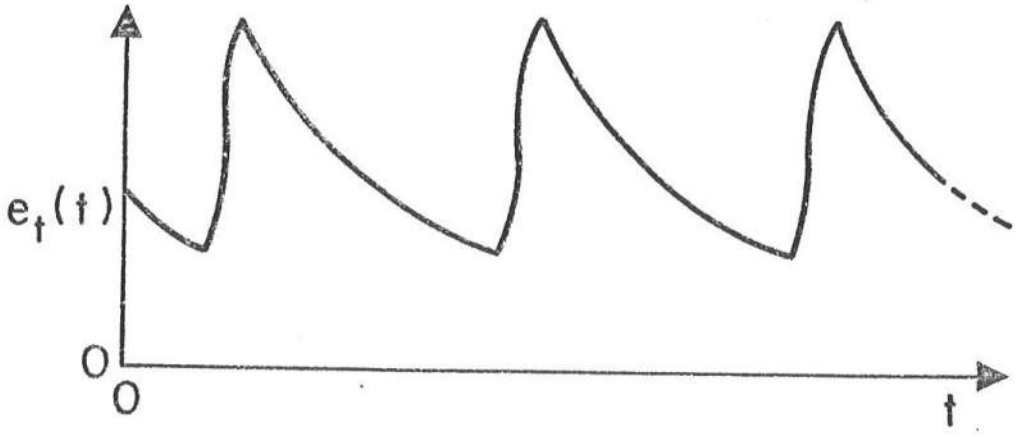

C) TURBULENCE ENERGY DENSITY, $e_t(t)$ FOR SMALL DECAY, β

FIGURE 15 Idealized Considerations of Turbulence Production and Density in the Surf Zone

it is possible to obtain solutions to Eq. (33) for assumed values of V, $\mathcal{D}_3$ and β, a meaningful solution of the problem of energetics in the surf zone requires further experimental and theoretical investigation. Qualitatively, the solution for turbulent energy per unit volume must appear as shown in Figure 15-b for large β or 15-c for small β. The peak turbulence level is probably governing from the standpoint of bottom stability.

It is possible to obtain a functional dependence of $\mathcal{D}_3$ on sediment characteristics by noting that the stability of a sediment particle can be expressed in terms of its submerged weight, W_s

$$W_s = B_1(\rho_s - \rho_w)\, g\, \frac{\pi D^3}{6} \tag{34}$$

where B_1 is a shape factor. The forces that are effective in dislodging the particle are a combination of drag and lift forces, each having the form

$$F = B_2 \frac{\rho_w}{2} \frac{\pi D^2}{4} u_T^2 \tag{35}$$

where u_T represents the total water particle velocity consisting of the organized wave, u_w, and turbulent velocity, u'. The factor, B_2, incorporates a drag and/or lift coefficient. For purposes here, it is assumed that the turbulent water particle velocity component is much greater than that due to the organized wave motion.

It is noted that the fall velocity, w, of the sediment particle is a useful descriptor of its hydrodynamic properties and that the submerged weight may be expressed in terms of the fall velocity,

$$W_s = B_3 \frac{\rho_w}{2} \frac{\pi D^2}{4} w^2 \tag{36}$$

and $B_3 \simeq B_2$. Incipient instability occurs for a particular ratio of F and W_s, depending on the angle of repose, ratio of lift to drag forces, etc. Since interest here is focused on a functional relationship, a fourth constant, B_4, may be introduced, i.e., incipient stability is given by

$$\frac{F}{W_s} = B_4 \tag{37}$$

It therefore follows that

$$u'^2 \alpha w^2 \tag{38}$$

and it is noted that w depends on shape, specific gravity and drag coefficient. However, since many beach sands are similar in shape and specific gravity, it is instructive to examine the effect of size, D only. If the velocities are such that Stoke's Law applies, then it can be shown that $w^2 \alpha D^4$. For Reynolds Number ranges in which the drag is quadratic, $w^2 \alpha D$. For spherical quartz particles in the diameter range 0.2 - 0.3 mm, and at realistic temperatures, $w^2 \alpha D^{2.5}$.

The functional relationship between $\mathcal{D}_3$ and sediment particle characteristics is obtained by assuming that the "effective" turbulent level is proportional to the rate of turbulence generation in the water column. This assumption is in approximate accord with Figure 15-b and if Figure 15-c is more representative of the phenomenon, then the wave period would be an important variable.

Based on the assumption above, the functional relationship of $\mathcal{D}_3$ vs. particle fall velocity is

$$\mathcal{D}_3(D) \propto w^2(D) \tag{39}$$

or for sediment diameters D_A and D_B,

$$\mathcal{D}_3(D_B) = \mathcal{D}_3(D_A) \frac{w^2(D_B)}{w^2(D_A)} \tag{40}$$

The quantitative relationship of $\mathcal{D}_3$ with sediment size is determined approximately by using the average A value of 0.150 which was obtained with m fixed at 0.67 and considering a representative diameter and temperature for all 502 profiles to be 0.3 mm and 20° C. Using Eq. (40) and the variation of fall velocity vs. diameter (Figure 16) the relationship of $\mathcal{D}_3$ with diameter D is as presented in Figure 12.

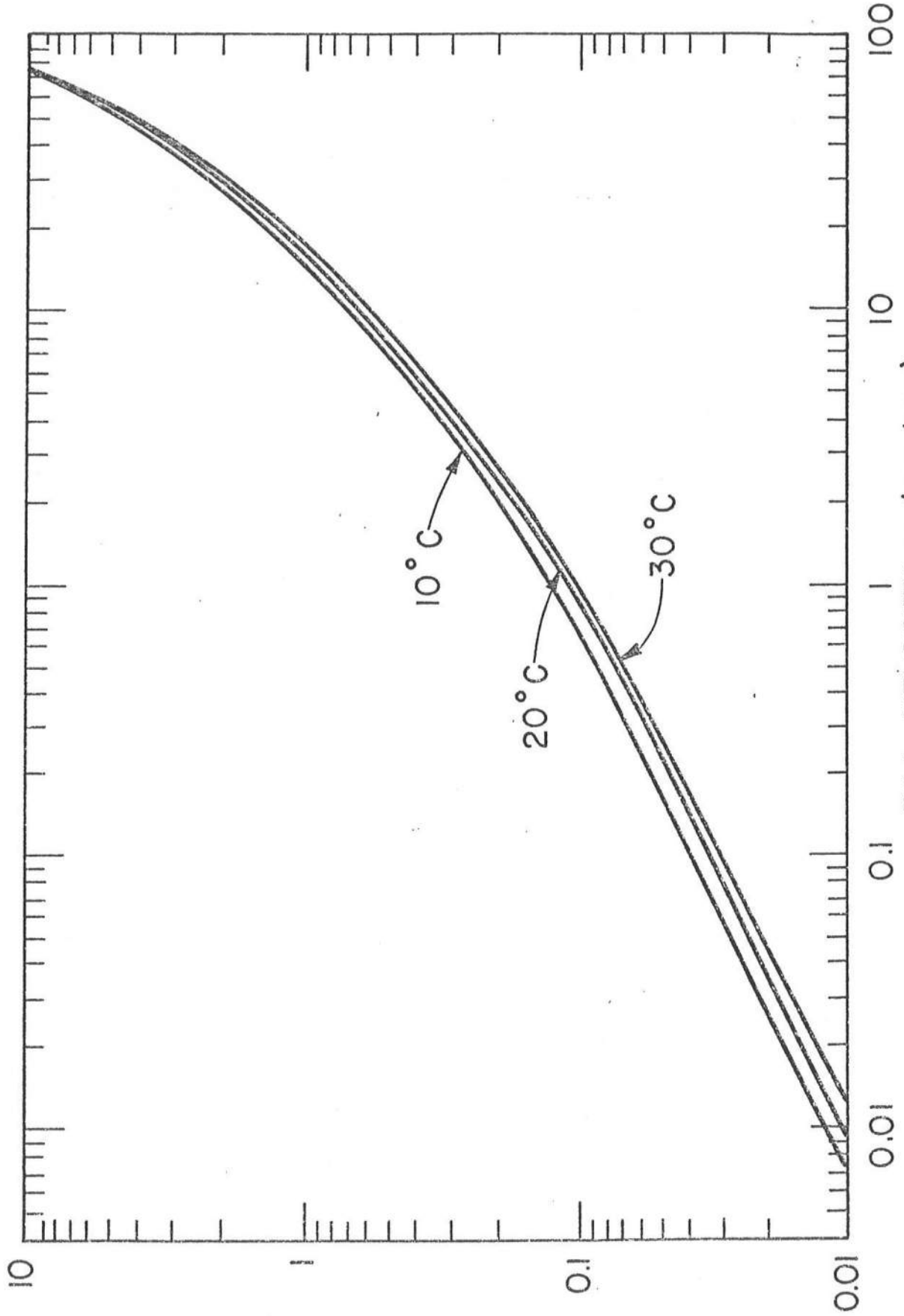

FIGURE 16 Fall Velocity Versus Diameter for Quartz Spheres